PHILOSOPHICAL TRANSACTIONS OF THE ROYAL SOCIETY A MATHEMATICAL, PHYSICAL & ENGINEERING SCIENCES

The Mineralogy and Crystal Chemistry of Deep-Sea Manganese Nodules, a Polymetallic Resource of the Twenty-First Century [and Discussion]

R. G. Burns, Virginia M. Burns and A. J. Easton

Phil. Trans. R. Soc. Lond. A 1977 **286**, 283-301
doi: 10.1098/rsta.1977.0118

Phil. Trans. R. Soc. Lond. A. **286**, 283–301 (1977) [283]
Printed in Great Britain

The mineralogy and crystal chemistry of deep-sea manganese nodules, a polymetallic resource of the twenty-first century

By R. G. Burns and Virginia M. Burns
Department of Earth and Planetary Sciences,
Massachusetts Institute of Technology, Cambridge, Massachusetts 02139, *U.S.A.*

The relatively high concentrations of cobalt, nickel, and copper in deep-sea manganese nodules, such as those occurring on the sea-bed beneath the north equatorial Pacific Ocean, indicate that these marine sediments are potential ore deposits. In order to explain the strong enrichments of Ni, Cu, and Co in the nodules, the crystal chemistries and structures of the host manganese oxide minerals must be understood. Over twenty manganese(IV) oxide minerals are known, but only three predominate in manganese nodules. They are todorokite, birnessite, and delta-MnO_2. All Mn^{IV} oxides contain edge-shared MnO_6 octahedra linked in diverse ways, leading to a hierarchy of structure-types somewhat resembling the classification of silicates. Todorokite is deduced to contain chains of edge-shared MnO_6 octahedra enclosing huge tunnels, thus resembling hollandite and psilomelane. Birnessite has a layered structure with essential vacancies in the sheets of edge-shared MnO_6 octahedra, while δ-MnO_2 is a disordered birnessite. The uptake of Co into manganese nodules involves replacement of low-spin Co^{3+} for Mn^{4+} ions in the structures, whereas Ni^{2+} and Cu^{2+} substitute for Mn^{2+} ions in octahedra located in the chains or between layers of edge-shared MnO_6 octahedra.

Introduction

This year, as well as marking the Centenary of the founding of the Mineralogical Society, is also the 100th anniversary of the ending of the three-year voyage of H.M.S. *Challenger*, in 1876, during which manganese nodules were first discovered. Ever since the publication of the cruise report of the Challenger Expedition (Murray & Renard 1891) and early descriptions of the minerals in these nodules (Murray & Irvine 1894), the origin and formation of deep-sea manganese nodule deposits have been the subjects of considerable speculation and debate (Glasby 1977). However, it is only in the past decade that the resource potential of marine manganese nodules has been fully appreciated (Mero 1965; Horn 1972; Morganstein 1973). Thus, nodules from the sea-floors underlying specific regions of the ocean, most notably the north equatorial Pacific defined by the coordinates: latitude 7° N to 16° N and longitude 117° W to 156° W, have been found to contain significant concentrations of the strategic metals nickel, copper, and cobalt (Mero 1965; Horn *et al.* 1973). Ocean mining technology and extractive metallurgical techniques have now advanced to the stage when harvesting of this vast sea-floor resource is both a feasible venture and an economic proposition (Sisselman 1975; Hubred 1975), despite political uncertainties originating from the Law of the Seas policies at the United Nations and from environmental protection agencies.

The decade of the 1970s also highlights the International Decade of Ocean Exploration (I.D.O.E.), a long-term cooperative programme of research and exploration of the oceans, which in the United States is managed by the National Science Foundation (N.S.F.). One

area of research sponsored by the N.S.F.–I.D.O.E.'s Seabed Assessment Program is the Manganese Nodule Project, in which a team of scientists spanning a wide range of disciplines – marine geology, chemistry, geochemistry, oceanography, sedimentology, geochronology, bacteriology, palaeontology, *and* mineralogy – is focusing efforts towards understanding the origin and distribution of those manganese nodule deposits containing sufficiently high concentrations of Ni, Cu, and Co to be potential ores (Burns 1975; Margolis & Burns 1976). One of the major aims of this research project is to elucidate the processes of uptake and enrichment of the transition elements in manganese nodules. This has brought mineralogy and crystal chemistry to the forefront of manganese nodule research; the constituent minerals not only influence mechanisms of adsorption and crystallization of the strategic metals into the nodules. but they also contribute to the authigenesis, growth, and structure of manganese nodules, Furthermore, the metallurgical processes used to extract the metals from manganese nodules mined from different localities on the sea-floor depend on the minerals present.

It is appropriate, therefore, 100 years after the discovery of manganese nodules and during the Centenary celebrations of the Mineralogical Society, to outline the current state of manganese oxide mineralogy and to point to future directions of research on the mineralogy of a submarine ore deposit which will be exploited during the 21st century.

Constituents of manganese nodules

The characterization of the phases constituting manganese nodules has necessitated a broad-minded view of what constitutes a mineral (Burns & Burns 1977*a*). The classical definition of a mineral as a naturally-occurring, *inorganically* produced, solid possessing a *characteristic chemical composition* or a limited range of compositions and a *systematic three-dimensional atomic order* must be expanded when referring to the minerals found in manganese nodules. This is demonstrated in the following description of the constituents of manganese nodules.

Manganese nodules are not monominerallic. Instead, they consist of a complex mixture of materials, including crystallites of several minerals of detrital and authigenic origins, organic and colloidal matter, and igneous and metamorphic rocks in varying stages of degradation. Some of the constituents of manganese nodules appear to be essential for the nucleation and growth of the component minerals. In most cases, the concretions have a nucleus which may be pumice, altered basaltic fragments or glass, clays or tuffaceous material, or the hard parts of organisms (e.g. sharks' teeth, whale bones, globigerina or radiolaria or diatom tests, coral, etc.), or fragments of older manganese nodules. Recent observations with the scanning electron microscope have revealed that mineralization occurs inside and on the outer surfaces of micro-organisms trapped within manganese nodules (Greenslate 1974*a*, *b*; Dugolinsky & Margolis 1976; Burns & Burns 1977*b*). Thus, some of the phases of manganese nodules may be *organically* produced (Graham & Cooper 1959; Erhlich 1963; Sorokin 1972).

The minerals in manganese nodules are fine-grained and intimately intergrown, giving rise to complex internal textures (Sorem & Foster 1972). Such heterogeneities and complicated internal structures make it very difficult to characterize the very small crystallites in manganese nodules. It is extremely difficult to extract a homogeneous, single-phase mineral sample from a manganese nodule for mineralogical studies. This has led to ambiguities over mineral identifications in manganese nodules by X-ray diffraction analysis. The particle sizes of crystallites are frequently 100 nm or less, and often smaller than 10 nm, so that coherent scattering of

PHILOSOPHICAL TRANSACTIONS OF THE ROYAL SOCIETY A MATHEMATICAL, PHYSICAL & ENGINEERING SCIENCES

X-rays from the lattice planes is improbable. Thus, the solids appear to be amorphous or to give broad, diffuse reflexions in X-ray diffraction patterns. Therefore, delineating between a cryptocrystalline mineral and an amorphous mineraloid by X-ray methods is arbitrary in the absence of long-range crystallographic ordering and when defects and vacancies occur in the crystal structures. As a result, information on dimensions and shapes of cryptocrystalline minerals is particularly important for elucidating the mineralogy of manganese nodules. Recently, significant progress has been made in identifying and deducing the crystal structures of the minerals in manganese nodules from scanning electron microscopy (s.e.m.), transmission electron microscopy (t.e.m.), and electron diffraction measurements on corroborative synthetic phases and terrestrial mineral analogues. Some of these results are discussed below.

Another problem encountered in manganese nodule mineralogy is to be able to distinguish between authigenic and detrital minerals included in the nodules, particularly the clay, zeolite, feldspar, silica, and iron oxyhydroxide phases. These may have been derived from terrigenous sources in suspension in seawater, or originated from detrital or secondary minerals in sediment layers trapped in the nodules, or recrystallized *in situ* inside the nodules.

Most interest centres on the oxide phases of manganese and iron in the nodules, because microchemical analyses by electron microprobe have demonstrated that Ni, Cu, and Co are associated with Fe and Mn (Burns & Fuerstenau 1966; Cronan & Tooms 1968; Ostwald & Frazer 1973). Confusion exists in the literature on manganese nodules over the nomenclature of the constituent manganese and iron oxide phases. This is attributable to the minute grain size of some of the phases, which not only makes them apparently amorphous to X-rays, but also has rendered X-ray determinations of their crystal structures impossible. Attempts have been made to correlate the nodule phases with terrestrial minerals on the one hand, and with products of synthesis on the other. As a result, at least three classification schemes exist in the literature on manganese nodules, leading to ambiguities between variously named species. These problems are discussed below.

Another problem highlighted by manganese nodules is that the crystal structures of the major minerals are characterized by numerous defects, essential vacancies, extensive atomic substitution, and pronounced cation exchange properties. These phenomena not only lead to non-stoichiometry, but detract from long-range ordering, making structure determinations of host minerals extremely difficult. These properties, which are the bane of classical mineralogy, are also discussed later.

Since manganese nodules form in oxidizing environments, the mineralogy of the nodules is dominated by hydrated oxides and oxyhydroxides of manganese(IV) and iron(III). Some of these minerals are described in the following sections.

Oxide minerals of manganese and iron

Manganese and iron form a large number of compounds with oxygen. These range from refractory anhydrous phases to hydrated minerals stable at low temperatures in aqueous environments. Although oxides such as jacobsite ($MnFe_2O_4$), α-vredenburgite [$(Mn, Fe)_3O_4$], hausmannite (Mn_3O_4), bixbyite [α-$(Mn, Fe)_2O_3$], partridgeite (α-Mn_2O_3), and braunite ($Mn^{2+}Mn^{3+}{}_6O_8.SiO_4$) are formed when ferromanganese nodules are heated to high temperatures and may be important in some extractive metallurgical processes, they are not important *per se* in manganese nodules which form at low temperatures in aerated aqueous environments.

More than twenty naturally-occurring oxide phases containing tetravalent manganese are currently recognized as valid mineral species (Burns & Burns 1977*a*). The more significant manganese(IV) oxide minerals are listed in table 1, together with available crystallographic data and current information on chemical compositions and crystal structures. Similar data for the oxide hydroxide minerals of Mn(III) and Fe(III) are given in table 2.

TABLE 1. SELECTED MANGANESE(IV) OXIDE MINERALS†

mineral	formula	crystal class (space group)	cell parameters pm	structure-type (isostructural compounds)
pyrolusite	β-MnO_2	tetragonal ($P4_2/mn2$)	$a_0 = 439$; $c_0 = 287$	rutile
‡ramsdellite	MnO_2	orthorhombic (Pbnm)	$a_0 = 453$; $b_0 = 927$; $c_0 = 287$	ramsdellite (diaspore, goethite†)
‡nsutite	(Mn^{2+}, Mn^{4+}) $(O, OH)_2$	hexagonal	$a_0 = 965$; $c_0 = 443$	pyrolusite + ramsdellite intergrowths
hollandite	$(Ba, K)_{1-2}$ $Mn_8O_{16}.xH_2O$	tetragonal (I4/m)	$a_0 = 996$; $c_0 = 286$	hollandite (cryptomelane, manjirōite, coronadite, α-MnO_2, akaganéite)
cryptomelane	K_{1-2} $Mn_8O_{16}.xH_2O$	tetragonal (I4/m)	$a_0 = 984$; $c_0 = 286$	hollandite
‡psilomelane	$(Ba, K, Mn, Co)_2$ $Mn_5O_{10}.xH_2O$	monoclinic (A2/m)	$a_0 = 956$; $b_0 = 288$; $c_0 = 1385$; $\beta = 92° 30'$	psilomelane
‡todorokite ('10 Å manganite') (buserite)	(Na, Ca, K, Ba, Mn^{2+}) $Mn_3O_7.xH_2O$	monoclinic	$a_0 = 975$; $b_0 = 3849$; $c_0 = 959$; $\beta = 90°$	unknown
lithiophorite	$[Mn_5^{4+}Mn^{2+}O_{12}].$ $[Al_4Li_2(OH)_{12}]$	monoclinic (C2/m)	$a_0 = 506$; $b_0 = 870$; $c_0 = 961$; $\beta = 100° 7'$	lithiophorite
chalcophanite	$ZnMn_3O_7.3H_2O$	triclinic ($P\bar{1}$)	$a_0 = 754$; $b_0 = 754$; $c_0 = 822$; $\alpha = 90°$; $\beta = 117° 12'$; $\gamma = 120°$	chalcophanite
synthetic birnessite ('7 Å manganite')	$Na_4Mn_{14}O_{27}.9H_2O$	orthorhombic	$a_0 = 854$; $b_0 = 1539$; $c_0 = 1426$	incompletely determined
‡natural birnessite	(Ca, Na) $(Mn^{2+}, Mn^{4+})_7O_{14}.xH_2O$	unknown	—	not determined
‡δ-MnO_2	(Mn, Co^{3+}) $Mn_6O_{13}.xH_2O$	hexagonal	—	disordered birnessite ($FeOOH.xH_2O$)‡

† Selected data from Burns & Burns (1977*a*).
‡ Reported in manganese nodules.

MINERALOGY OF MANGANESE NODULES

Many of the Mn^{IV} oxide minerals listed in table 1 have been positively identified or tentatively suggested to occur in a variety of manganese nodules. These are designated in the footnotes to tables 1 and 2.

Originally, Murray & Renard (1891), on the basis of chemical analysis, concluded that the nodules from the Challenger Expedition consisted of wad or bog manganese ore, which they noted were impure varieties of manganese oxides related to the mineral psilomelane. The classic studies of Buser (Buser & Grütter 1956; Buser 1959) led to the terminology of '10 Å

manganite', '7 Å manganite', and 'delta-MnO_2' for three different crystalline phases in manganese nodules giving distinctive X-ray powder diffraction patterns that could be correlated with those of certain synthetic manganese oxides. This terminology has long been considered unsatisfactory because it leads to confusion with the mineral manganite (γ-MnOOH), which has not been positively identified in manganese nodules. Recent studies of these synthetic phases (Giovanoli *et al.* 1970*a*, *b*; 1971) produced the alternative nomenclature scheme: sodium manganese(II, III) manganate(IV) hydrate, sodium manganese(II, III), manganate(IV), and manganese(III) manganate(IV) for the '10 Å manganite', '7 Å manganite', and

TABLE 2. SELECTED OXIDE HYDROXIDE MINERALS OF MANGANESE(III) AND IRON(III)†

mineral	formula	crystal class (space group)	cell parameters pm	structural-type (isostructural compounds)
groutite	α-MnOOH	orthorhombic (Pbnm)	$a_0 = 456$; $b_0 = 1070$; $c_0 = 285$; $z = 4$	diaspore (ramsdellite, goethite)
feitknechtite	β-MnOOH	hexagonal ($P\bar{3}ml$)	$a_0 = 332$; $c_0 = 471$; $z = 1$	pyrochroite
manganite	γ-MnOOH	monoclinic ($B2_1/d$)	$a_0 = 888$; $b_0 = 525$; $c_0 = 571$; $\beta = 90°$; $z = 8$	manganite (distorted rutile)
‡goethite	α-FeOOH	orthorhombic (Pbnm)	$a_0 = 465$; $b_0 = 1002$; $c_0 = 304$; $z = 4$	diaspore (ramsdellite, groutite)
‡akaganéite	β-FeOOH	tetragonal (I4/m)	$a_0 = 1048$; $c_0 = 3028$; $z = 8$	hollandite
lepidocrocite	γ-FeOOH	orthorhombic (Amam)	$a_0 = 388$; $b_0 = 1254$; $c_0 = 307$; $z = 4$	boehmite
‡ferrihydrite	$Fe_2O_3.xH_2O$	amorphous		

† Selected data from tabulation from Burns & Burns (1977*a*).
‡ Reported in manganese nodules.

'δ-MnO_2' phases, respectively. A third nomenclature scheme, based on the close agreement of certain lines in the X-ray powder patterns of manganese nodules with those of the terrestrial minerals todorokite and birnessite (Manheim 1965), is now generally adopted (Burns & Burns 1977*a*). Recently, it was recommended that name the δ-MnO_2 be retained for a disordered birnessite phase having minimal structural periodicity (Burns *et al.* 1974). It should be noted, however, that the validity of todorokite as a homogeneous phase is currently under debate. Electron diffraction measurements of synthetic phases have been interpreted (Giovanoli *et al.* 1971) as indicating that todorokite is a mixture of primary buserite ('10 Å manganite') partly dehydrated to birnessite and partly reduced to manganite (γ-MnOOH). Such degradation of todorokite is difficult to envisage in the aerated aqueous environment in which nodules occur. The γ-MnOOH crystals are extremely small so as to be undetectable by X-ray diffraction analysis (Giovanoli & Burki 1975). Synthetic buserite was accepted as a new mineral in place of the '10 Å manganite' phase in manganese nodules in 1970 by the I.M.A. Commission on New Minerals (Hey & Embrey 1974). Several mineralogists believe that much stronger evidence is required before the naturally occurring mineral todorokite is discredited in favour of the unstable synthetic phase buserite (Burns *et al.* 1974). It is confusing to find todorokite so widely and voluminously distributed in the lithospheric and oceanic crust giving reproducible X-ray powder patterns with no evidence of the strongest lines for manganite and birnessite. Further work is required to resolve the todorokite–buserite problem. Other

PHILOSOPHICAL TRANSACTIONS OF THE ROYAL SOCIETY A MATHEMATICAL, PHYSICAL & ENGINEERING SCIENCES

manganese(IV) oxide minerals reported in manganese nodules, in addition to the dominant phases todorokite, birnessite, and δ-MnO_2, include ramsdellite, nsutite, and psilomelane (Burns & Burns 1977*a*).

The iron-bearing minerals in manganese nodules are usually amorphous to X-rays. Again, there is confusion and misidentification in the literature of the hydrated iron oxide–hydroxide phases occurring in nodules (Burns & Burns 1977*a*). It is now generally accepted that the most common iron-bearing phases in nodules are goethite and material variously called 'amorphous $Fe(OH)_3$', 'iron(III) oxide hydrate gel', 'colloidal ferric species', and 'hydrated ferric oxide polymer', which may be identical with the new mineral ferrihydrite (Chukhrov *et al.* 1973). The crystallites of this mineral rarely exceed 10 nm, accounting for its being amorphous to X-rays.

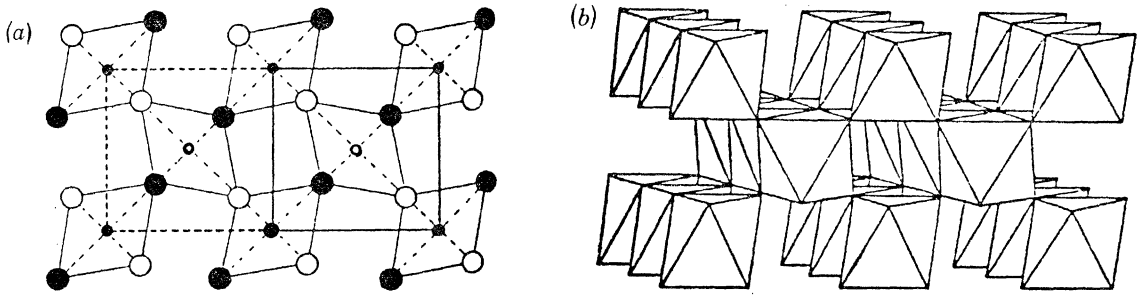

FIGURE 1. The pyrolusite structure. (*a*) Projection on to (001); closed circles, atoms at zero level; open circles, atoms at level 1/2*c* (after Byström 1949). (*b*) The single chains of edge-shared [MnO_6] octahedra parallel to *c* (after Clark 1972). ○ ●, Mn; ○ ●, O.

CRYSTAL STRUCTURES OF THE MINERALS IN MANGANESE NODULES

The authigenesis of manganese nodules and the uptake of certain metals into the ferromanganese oxide phases is fundamentally controlled by the crystal structures of the host minerals and the crystal chemistries of the substituent cations. An area of active research is to deduce the structures of host manganese(IV) oxide and iron(III) oxide–hydroxide phases of manganese nodules. Most of the structural information is derived from crystal morphologies observed with scanning electron microscopes and electron diffraction measurements of synthetic analogues. In order to arrive at reasonable crystal structures of the minerals in manganese nodules, it is essential to establish first structural correlations between manganese(IV) oxide minerals of known crystal structure.

Structural correlations between manganese(IV) oxides

Available crystal structural data for the various manganese oxides and oxyhydroxides indicate that there is a hierarchy of structure-types, somewhat resembling the classification of common rock-forming silicates. Thus, as with the independent, chain, ring, framework, and layer silicates, which are related to one another by different linkages of the fundamental [SiO_4] tetrahedral units, so too there are different ways of connecting the basic [MnO_6] or [$Mn(O, OH)_6$] octahedra in the manganese oxides. In the structures of manganese oxide minerals, the linkages occur by edge-sharing of the [MnO_6] octahedra.

(i) *Chain structures.* The basis for describing the crystal structures of manganese(IV) oxides and oxyhydroxides is the pyrolusite (β-MnO_2) structure. It has the rutile (TiO_2) structure,

PHILOSOPHICAL TRANSACTIONS OF THE ROYAL SOCIETY A MATHEMATICAL, PHYSICAL & ENGINEERING SCIENCES

in which every metal atom is surrounded by six oxygen atoms located at the vertices of a distorted octahedron with Mn at the centre. The [MnO_6] octahedra share edges to form single chains of octahedra extending along the c crystallographic axis. All the octahedra are equivalent, and the average Mn–O distance is 188 pm. The unit cell c_0 dimension (287 pm) represents the Mn–Mn internuclear distance across the shared octahedral edge and, as may be noted from table 1, is a common cell parameter found in manganese(IV) oxide mineralogy. The chains of [MnO_6] are crosslinked with neighbouring chains through corner-sharing of oxygen atoms of adjacent octahedra to give tetragonal symmetry to pyrolusite. The crystal structure of pyrolusite is shown in figure 1. The single chains of linked [MnO_6] octahedra in pyrolusite thus somewhat resemble the single [SiO_4] chains in pyroxenes.

Manganite (γ-MnOOH) has a structure resembling pyrolusite. The four oxygens in the planes of edge-shared [MnO_6] octahedra are closer (Mn–O = 187–198 pm) to the central Mn(III) atom than are the two apical oxygens (Mn–O = 220–233 pm). This is the result of the Jahn–Teller effect in Mn^{3+} ions. Hydrogen-bonding occurs between the OH groups in edge-shared octahedra in one chain and the apical (corner-shared) oxygens belonging to adjacent chains. The pronounced basal cleavage of manganite results from the hydrogen-bonding.

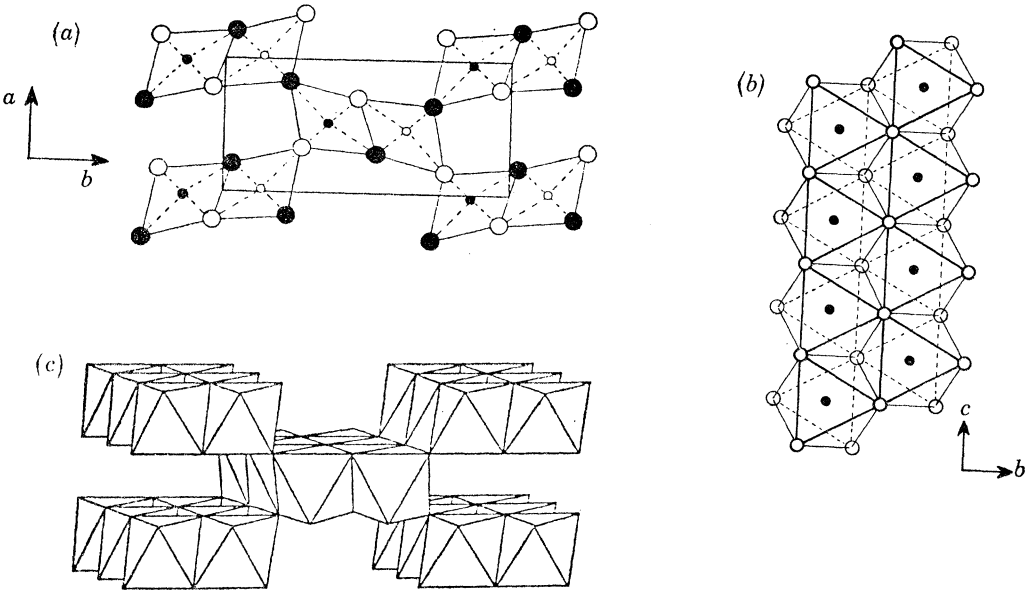

FIGURE 2. The ramsdellite structure. (*a*) Projection on to (001); open circles, atoms at level 1/4*c*; shaded circles, atoms at level 3/4*c* (after Byström 1949). (*b*) A double-chain of [MnO_6] octahedra running along *c* (after Byström 1949). (*c*) The double-chains of edge-shared [MnO_6] octahedra parallel to *c* (after Clark 1972). ○ ●, Mn; ○ ●, O.

Ramsdellite (MnO_2) is built up of alternating double chains of linked [MnO_6] octahedra (figure 2) (Byström 1949), and, therefore, resembles the double chains of amphiboles in silicate mineralogy. The octahedra are linked together by sharing opposite edges, thus producing continuous pyrolusite-like chains along the c axis. Two such chains are cross-linked by edge-sharing, one chain being displaced by $\frac{1}{2}c_0$ with respect to the other, so that an octahedron from one chain shares an edge with each of two octahedra from the other chain. The double chains of linked octahedra are further cross-linked to adjacent double chains through corner-sharing of oxygen atoms, to give orthorhombic symmetry to ramsdellite. These features are illustrated

in figure 2. All octahedra have identical configurations with an average Mn–O distance of 189 pm.

The nsutite or γ-MnO_2 group consists of irregular structural intergrowths between pyrolusite and ramsellite units. The alternating c-axis chain segments of the basic single and double chain units are random, so that no regular periodicity or superstructure is apparent. The lattice disorder causes nsutites and synthetic γ-MnO_2 phases to have extensive defects, vacancies, and non-stoichiometric properties. These factors, together with the small crystallite sizes of natural and synthetic phases, therefore give rise to an infinite number of X-ray powder diffraction patterns, as well as the frequently observed asymmetric and selective line broadening for nsutites.

Groutite (α-MnOOH) is isostructural with ramsdellite and consists of double chains of linked [Mn(O, OH)$_6$] octahedra, in which hydrogen-bonding also plays a significant rôle. Goethite (α-FeOOH) is also isostructural with ramsdellite.

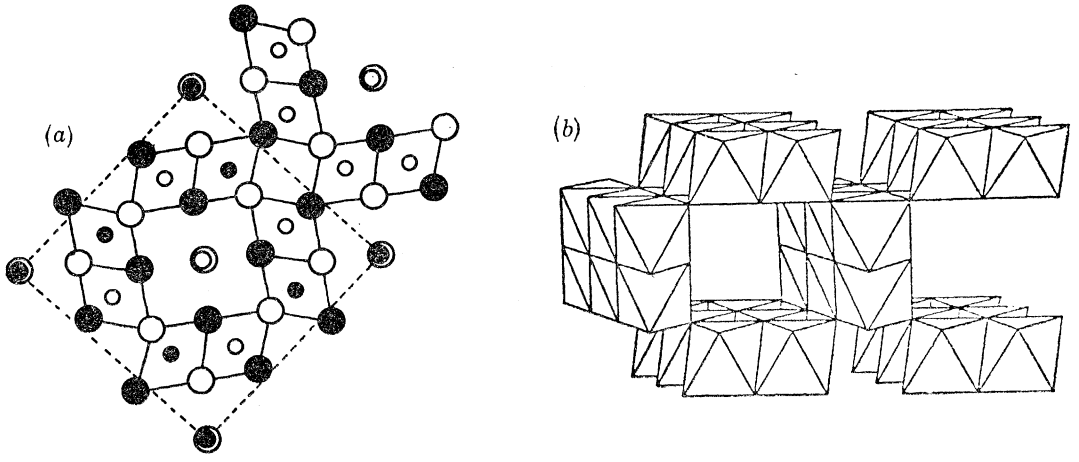

FIGURE 3. The hollandite structure-type. (*a*) The structure of hollandite projected onto (001); open circles, atoms at zero level; shaded circles, atoms at level 1/2c (after Byström & Byström 1950). (*b*) The framework structure of hollandite, showing tunnels between double-chains of edge-shared [MnO_6] octahedra parallel to c (after Clark 1972). ○ ●, Mn; ○ ●, O; ◎ ⊙, Ba, K, Pb, Na, or H_2O.

(ii) *Ring or framework structures.* The structure of α-MnO_2 and minerals of the cryptomelane–hollandite group, which is shown in figure 3, is based on the ramsdellite structure (Byström & Byström 1950). The [MnO_6] octahedra again share edges and form double chains running along the c axis. The octahedra of the double chains share corners with adjacent double chains to give a three-dimensional framework with pseudo-tetragonal symmetry (figure 3). This produces a large cavity which accommodates H_2O as well as the large monovalent and divalent cations, such as Ba^{2+}, Pb^{2+}, K^+, and Na^+ in hollandite, coronadite, cryptomelane, and manjirōite, respectively. Each large cation is surrounded by 8 oxygen atoms situated at the corners of a slightly distorted cube (e.g. Ba–O distances in hollandite are 274 pm to these 8 oxygens) and four other oxygens (Ba–O = 331 pm) at the corners of a square at the same level along the c axis as the large cation. The c_0 dimension (286 pm) again represents the Mn–Mn internuclear distance. Disordering of K^+, Ba^{2+}, etc., and H_2O occurs in the cavities, which are probably no more than half-filled, otherwise unfavourable cation repulsions would occur when Ba^{2+}–Ba^{2+}, K^+–K^+, etc., pairs are as close as 286 nm. On the other hand, signi-

ficant amounts of H_2O, K^+, NH_4^+, etc., are necessary to prevent collapse of the structure of synthetic α-MnO_2, otherwise submicroheterogenieties are formed in which regions of pyrolusite and ramsdellite are interdispersed and coexist with regions of α-MnO_2 in the same crystal. Natural hollandites and cryptomelanes, however, appear to be stable up to very high temperatures because they retain the Ba^{2+} and K^+ ions.

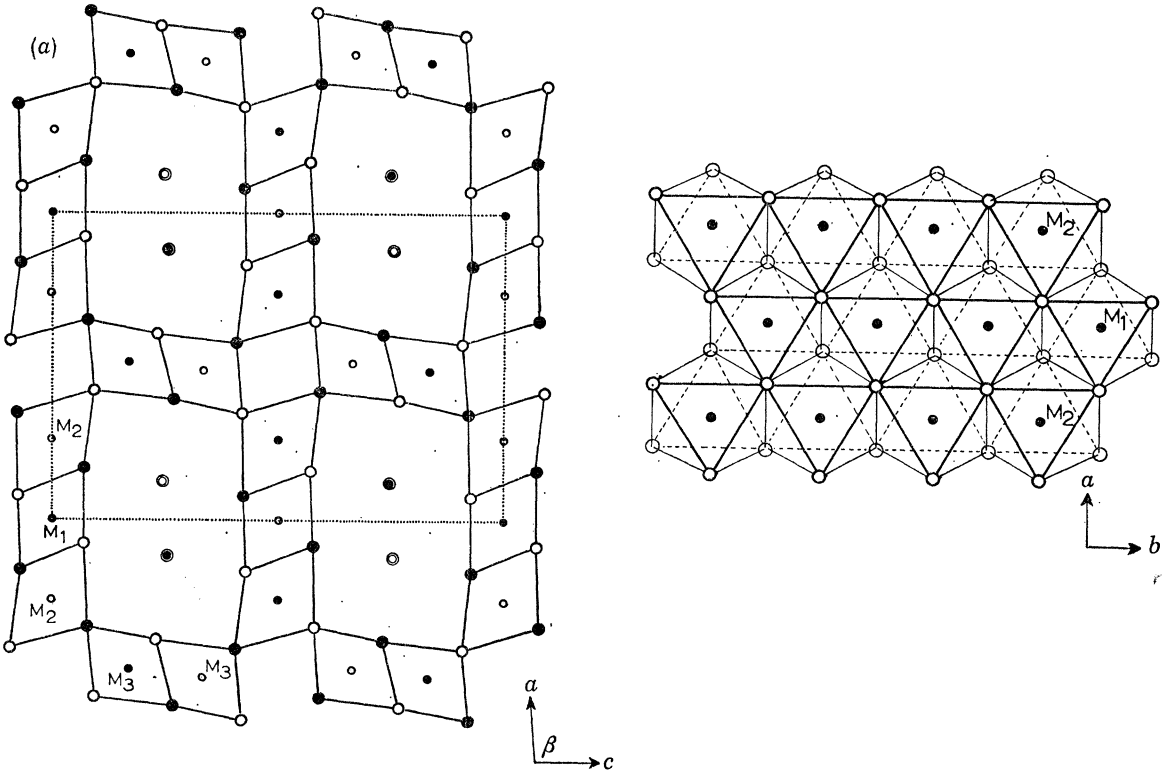

FIGURE 4. The psilomelane structure (after Wadsley 1953). (*a*) Projection on to (010), showing four linked tunnels. The unit cell is shown by broken lines. Open circles, atoms at zero level; shaded circles, atoms at level 1/2*b*. ○, ●, Mn; ○ ●, O; ◎ ⊙, Ba, K, or H_2O. (*b*) A treble-chain of [MnO_6] octahedra parallel to the *b* axis.

A significant property of the sieve-like structure of hollandite is that it displays pronounced cation exchange properties. In order to maintain a charge balance in the structure accommodating the large exchangeable cations (Ba^{2+}, K^+, Na^+, Pb^{2+}), the linked [MnO_6] octahedra must contain some OH groups, cation vacancies, or a proportion of the manganese in oxidation states (e.g. Mn^{2+}, Mn^{3+}) lower than Mn^{IV}. This is reflected in the average metal–oxygen distance of the [MnO_6] octahedra, 198 pm, which is significantly larger than the mean Mn–O distance in pyrolusite (188 pm), reflecting the larger ionic radii of Mn^{2+} and Mn^{3+}. The non-stoichiometry and local charge-balancing of vacancies in the [MnO_6] octahedra by the large cations in the tunnels or voids are important factors in the hollandite structure.

Akaganéite, β-FeOOH, is isostructural with the hollandite group. Its structure accommodates H_2O molecules and OH^-, Cl^-, F^-, SO_4^{2-}, and NO_3^- ions in the large cavities. Synthetic β-FeOOH has spindle-shaped crystals which appear under the electron microscope to be built up of parallel needles or rod-like sub-crystals packed into an orthogonal array. The rods are typically 6 nm square in section and up to 600 nm in length. When assembled into regular parallel bundles, crystals about 60 nm wide with tapered ends are observed. Evidence suggests

that these rods are hollow, their internal diameter being about 3 nm (Gallagher 1970). The significance of this structure-type in relation to todorokite is discussed later.

Psilomelane has a structure related to that of hollandite (Wadsley 1953). It consists of *treble* chains of MnO_6 octahedra joined by double (ramsdellite-like) chains to form a series of tunnels or tubes running in the direction of the b axis (figure 4). The b_0 dimension (288 pm) of psilomelane, therefore, corresponds to c_0 of pyrolusite, ramsdellite, and hollandite. The tunnels are occupied by Ba^{2+}, K^+ ions and H_2O molecules. Thus, the psilomelane structure resembles the hollandite structure, to which it decomposes at high temperatures. Psilomelane also has cation exchange properties and requires some of the manganese to be in oxidation states lower than Mn^{IV} in order to balance the charge of the exchangeable large cations (Ba^{2+}, K^+). The psilomelane structure differs from the pyrolusite, ramsdellite, and hollandite structures described earlier by having *three* distinct octahedral sites. Two of them (the M_1 and M_3 sites) each have average metal–oxygen distances of 191 pm, which is significantly smaller than that (199 pm) of the third site (M_2), indicating that the M_2 site is enriched in the lower valence cations. These M_2-type sites of psilomelane provide a clue to the mechanism of uptake of Ni^{2+} and Cu^{2+} into todorokite in deep-sea manganese nodules.

(iii) *Layer structures*. An important mineral group in manganese nodules is the birnessite delta-MnO_2 group. Complete structure determinations have not been made for these phases, but they are known to possess layered structures.

The structural model for the manganese(IV) oxides with layered structures is chalcophanite, $ZnMn_3O_7.3H_2O$, the structure of which is illustrated in figure 5. The chalcophanite structure (Wadsley 1955) consists of single sheets of water molecules between layers of edge-shared [MnO_6] octahedra, with Zn atoms located between the water layer and oxygens of the [MnO_6] layer. The stacking sequence along the c axis is thus: –O–Mn–O–Zn–H_2O–Zn–O–Mn–O and the perpendicular distance between two consecutive [MnO_6] layers is about 717 pm. The water molecules are grouped in open double hexagonal rings, while vacancies exist in the layer of linked [MnO_6] octahedra, so that six out of every seven octahedral sites are occupied by manganese. Each [MnO_6] octahedron shares edges with five neighbouring octahedra and is adjacent to a vacancy (figure 5). The Zn atoms are located above and below the vacancies in the manganese layer and are coordinated to three oxygens of the [MnO_6] layer. Each Zn atom completes its coordination with three water molecules so as to form an irregular coordination polyhedron. The chemical compositions of natural chalcophanites differ significantly from the ideal formula, $Zn^{2+}Mn_3^{4+}O_7.3H_2O$. Not only is the water content variable, but there is a deficiency of Mn^{4+} ions and the number of cations usually exceeds 4 per formula unit. These trends indicate that some Mn^{2+} replaces Mn^{+4} in the linked octahedra, accounting for the larger average Mn–O distance of 195 pm (compared with 188 pm in pyrolusite or ramsdellite). Additional cations also occur in interstitial positions between the H_2O layers and oxygens of the [MnO_6] layers.

Lithiophorite also has a layer structure (Wadsley 1952), in which layers of edge-shared [MnO_6] octahedra alternate with layers of (Al, Li) $(OH)_6$ octahedra. The stacking sequence along the c axis is: –O–Mn–O–OH–(Al, Li)–OH–O–Mn–O, and two consecutive [MnO_6] layers are about 950 pm apart. Vacancies occurring in the sheets of linked [MnO_6] octahedra in the chalcophanite structure are not characteristic of the linked [MnO_6] octahedral layers of lithiophorite. Similarly, the ordered vacancies characteristic of the gibbsite, $Al(OH)_3$, structure are not found in the layer of linked [(Al, Li)(OH_6)] octahedra in lithiophorite. On

PHILOSOPHICAL TRANSACTIONS OF THE ROYAL SOCIETY A MATHEMATICAL, PHYSICAL & ENGINEERING SCIENCES

the other hand, substitution of Mn^{2+} for Mn^{4+} in the $[MnO_6]$ layers is required to maintain charge balance. Recent X-ray and electron diffraction studies of synthetic lithiophorite (Giovanoli *et al.* 1973) have led to the formulation $[(Mn_5^{4+}Mn^{2+}O_{12})^{2-}(Al_4Li_2(OH)_{12})^{2+}]$. A layer structure also occurs in the synthetic phases $CdMn_3O_8$ and Mn_5O_8 (Ostwald & Wampetich 1967). There are vacancies in the edge-shared $[MnO_6]$ containing Mn^{4+} ions. The Mn^{2+} and Cd^{2+} ions lie above and below the empty Mn^{IV} sites. Later, the rôle that such vacancies in the layers of linked $[Mn^{IV}O_6]$ octahedra play in the chemisorption of cobalt and other heavy metals onto Mn^{IV} oxides is discussed.

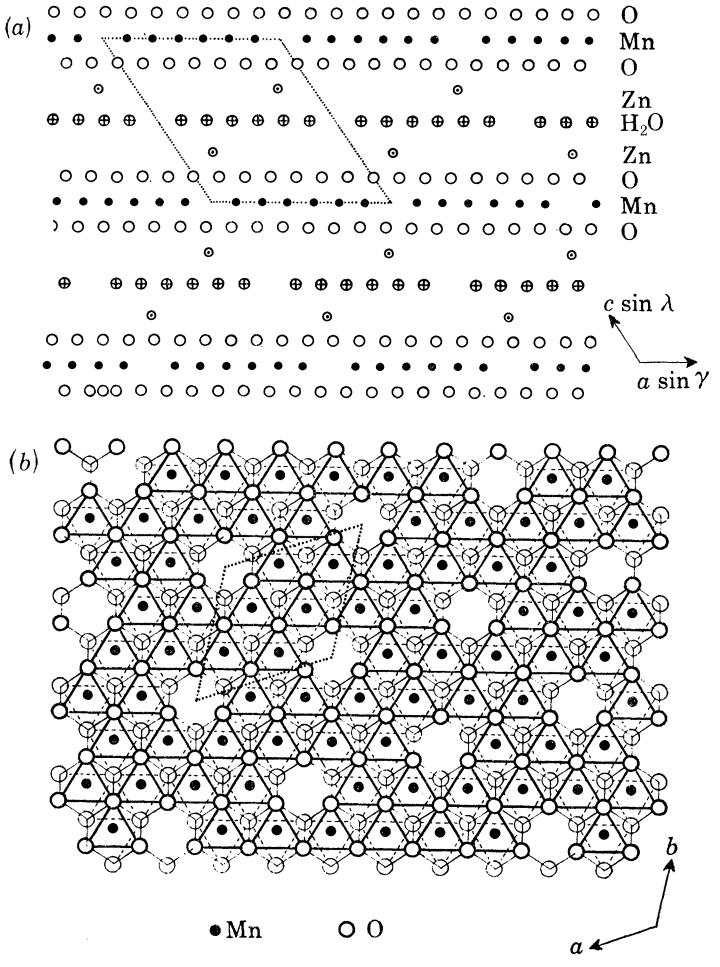

FIGURE 5. The chalcophanite structure (after Wadsley 1955). (*a*) Projection along the *b* axis. Vacancies in the Mn layers define the rhombus unit cell. Note that one out of every seven Mn positions is a vacancy. (*b*) The edge-shared $[MnO_6]$ layer viewed normal to the basal plane. The vacant octahedral sites at the origin are at the corners of a rhombus outlining the plane of the Mn atoms. Note that each Mn atoms is adjacent to a vacancy.

(iv) *Deductions on the birnessite structure.* Although the crystal structure of a natural birnessite has not been determined, information has been derived for synthetic compounds of the birnessite group from electron diffraction measurements (Giovanoli *et al.* 1970*a*, *b*). Platelets of synthetic $Na_4Mn_{14}O_{27}.9H_2O$ and $Mn_7O_{13}.5H_2O$ were deduced to have structures modelled on that of chalcophanite. Thus, sheets of water molecules and hydroxyl groups are located between layers of edge-shared $[MnO_6]$ octahedra separated by about 720 pm along the *c* axis.

One out of every six octahedral sites in the layer of linked [MnO_6] octahedra is unoccupied (compared with one out of seven in chalcophanite), and Mn^{2+} or Mn^{3+} ions are considered to lie above and below these vacancies. These low valency manganese ions are coordinated to oxygens in both the [MnO_6] layer and the (H_2O, OH) sheet. The position of sodium in the intermediate layer is uncertain. Projections of the lattice of $Na_4Mn_{14}O_{27}.9H_2O$ are shown in figure 6. Note that the unit cell of birnessite is determined by the location of essential vacancies in the edge-shared [MnO_6] layers.

The phase δ-MnO_2 is generally considered to be a disordered variety of birnessite. X-ray patterns of δ-MnO_2 typically contain only two broad diffuse lines at about 240 pm and

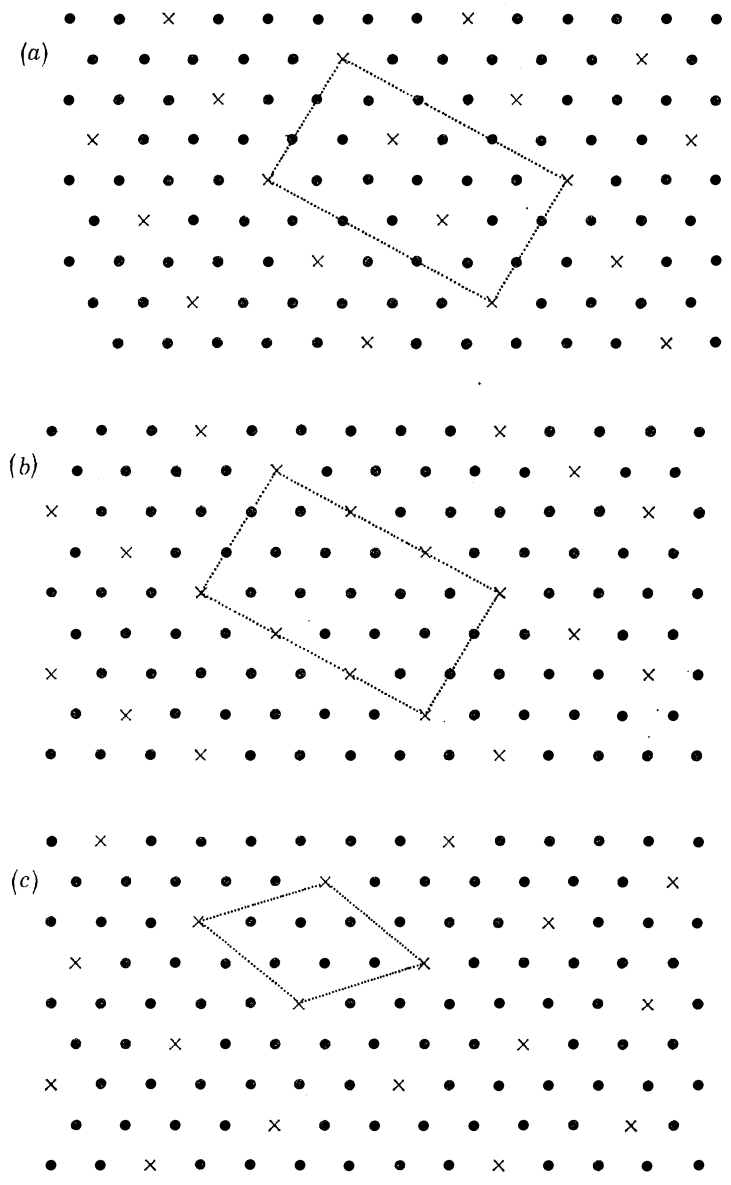

FIGURE 6. Projections of the structure proposed for synthetic birnessite, $Na_4Mn_{14}O_{27}.9H_2O$ (after Giovanoli *et al.* 1970*a*). The projections show Mn atoms only in the basal planes at zero level (*a*) and at about 720 pm along *c* (*b*). The different locations of vacancies in levels (*a*) and (*b*) necessitate doubling of the c_0 parameter. A comparable projection for reference (*c*).

PHILOSOPHICAL TRANSACTIONS OF THE ROYAL SOCIETY A MATHEMATICAL, PHYSICAL & ENGINEERING SCIENCES

142 pm with little or no suggestion of the additional lines at 700–720 pm and 350–360 pm, which are the diagnostic basal plane reflexions for birnessite. Synthetic birnessites (formerly called manganous manganite and '7 Å manganite') typically have surface areas in the range 30–50 $m^2\ g^{-1}$, which is almost an order of magnitude smaller than those of δ-MnO_2. Surface areas for a monatomic layer have been estimated to be about 720 $m^2\ g^{-1}$, so that the thickness of the two-dimensional δ-MnO_2 consists of fragments of the layers of edge-shared [MnO_6] octahedra with small periodicities of stacking along the *c* axis found in chalcophanite (figure 5) and birnessite. As a result, there is a high proportion of vacancies on exterior surfaces of δ-MnO_2 available for sorption of cations on each side and within the sheets of edge-shared [MnO_6] octahedra.

It is noteworthy that the habits of natural and synthetic birnessites correlate with the proposed layer structure. Thus, electron micrographs of natural (Brown *et al.* 1971; Woo 1973) and synthetic (Giovanoli *et al.* 1970*a*, *b*) birnessites show crystals with platy and lamellar habits, which differ significantly from the acicular habit of todorokite.

(v) *Deductions on the todorokite structure*. The crystal structure of todorokite has not been determined, mainly because single crystals suitable for a structural analysis have not been found. As noted earlier, there is evidence to suggest that the phase in manganese nodules called '10 Å manganite' (Buser 1959) corresponds to the terrestrial mineral todorokite. Buser & Grütter (1956) suggested that the '10 Å manganite' (todorokite) phase in manganese nodules is related structurally to lithiophorite, because prominent *d*-spacings around 960 pm and 480 pm for manganese nodules correspond to similar basal spacings in the X-ray powder diffraction pattern for lithiophorite. As a result, there is a widely held view that lithiophorite is the structural model for one of the dominant manganese oxide phases in manganese nodules. However, synthesis experiments of lithiophorite by Giovanoli *et al.* (1973) showed that substantial amounts of Na^+ or other cations cannot be substituted in the lithiophorite structure. They concluded that lithiophorite differs fundamentally from the 'buserite' (todorokite) group, the only similarities being the basal reflections around 952 pm and 474 pm and the Mn–Mn distances within the linked [MnO_6] octahedra.

A structural correlation of '10 Å manganite' (todorokite) with lithiophorite is unsatisfactory when crystal habits of terrestrial todorokites and lithiophorites are compared. Crystals of lithiophorite consist of laminae showing one perfect cleavage parallel to (001). This habit correlates with the layer structure determined for lithiophorite (Wadsley 1952). Todorokite specimens, on the other hand, consist of fibrous aggregates of small needle-shaped crystals, resembling many specimens of cryptomelane, hollandite, akaganéite, and psilomelane. Furthermore, electron micrographs of todorokite (Straczek *et al.* 1960) show that the crystals consist of narrow lathes or blades elongated along one axis (parallel to *b*) and showing *two* perfect cleavages parallel to the (001) and (100) planes. Minerals of the hollandite and psilomelane groups also show two perfect mutually perpendicular cleavages at right angles to the elongation of the acicular crystals. These resemblances suggest that todorokite has a crystal structure resembling those of hollandite and psilomelane and not that of lithiophorite. This correlation is further borne out when comparisons are made between the cell parameters summarized in table 1. If todorokite does have a framework structure analogous to those of hollandite or psilomelane, then it is possible that Mn^{2+} and Mn^{4+} ions occur together in chains of edge-shared [MnO_6] octahedra which are stacked in such a manner so as to be able to accommodate large cations and H_2O molecules.

PHILOSOPHICAL TRANSACTIONS OF THE ROYAL SOCIETY A MATHEMATICAL, PHYSICAL & ENGINEERING SCIENCES

Another clue to the structure-type of todorokite comes from recent studies of titanium(IV) oxide phases. Titanium forms several mixed oxide phases with acicular habits, the structures of which contain double (ramsdellite-type) or treble (psilomelane-type) chains of edge-shared octahedra providing large tunnels which accommodate large cations such as Na^{+} and Ca^{2+}. Examples include $NaAlTi_3O_8$ with the hollandite structure, $Na_4Mn_4Ti_5O_{18}$, $NaAl_5Ti_2O_{12}$,

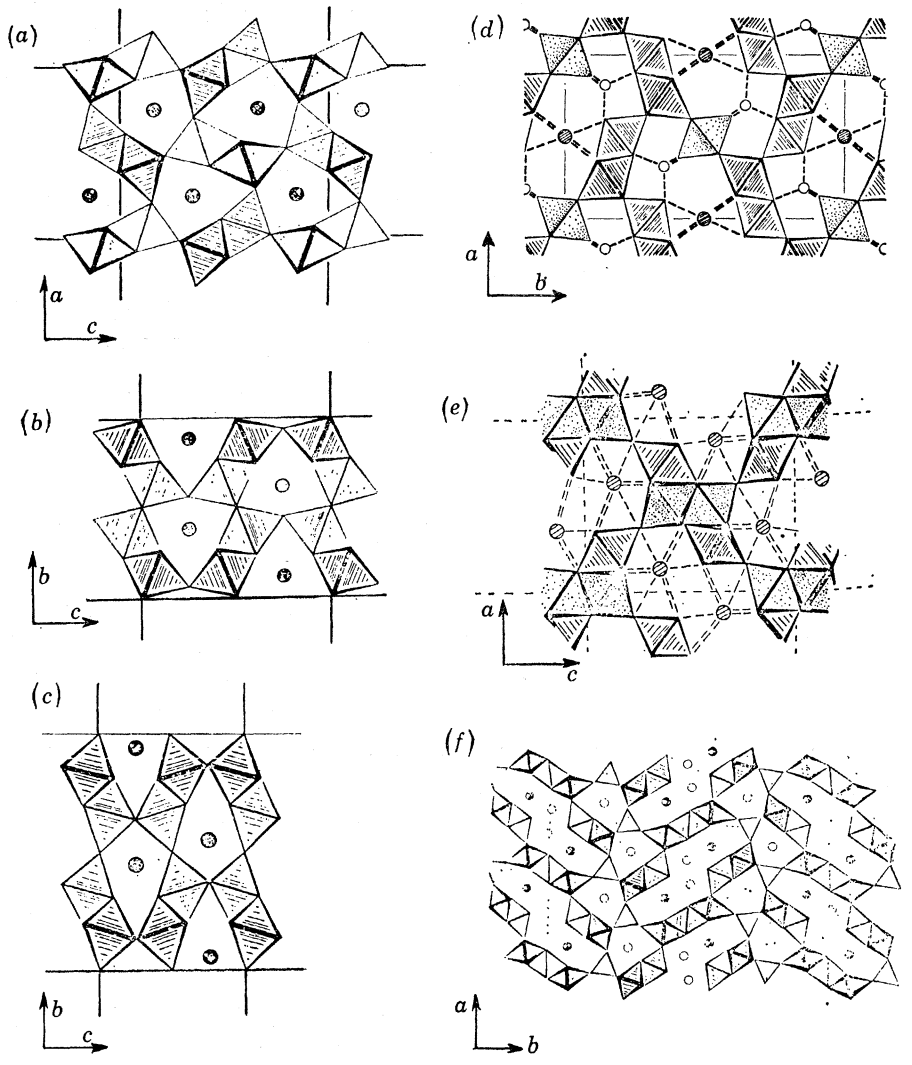

FIGURE 7. Structures of selected Ti^{IV} oxides showing double and treble chains of edge-shared octahedra (after Mumme 1968; Mumme & Wadsley 1967; Mumme & Reid 1968). (*a*) $NaFeTiO_4$; (*b*) $CaTi_2O_4$; (*c*) Hypothetical alternative to $CaTi_2O_4$; (*d*) $NaTi_2Al_5O_{12}$; (*e*) $Na_xFe_xTi_{2-x}O_4$; (*f*) $Na_4Mn_4Ti_4O_{18}$.

$NaFeTiO_4$, and $Na_xFe_xTi_{2-x}O_4$ (Mumme 1968; Mumme & Wadsley 1967; Mumme & Reid 1968), and are illustrated in figure 7. The Ti^{IV} oxides appear to have higher thermal stabilities than isostructural Mn^{IV} oxides, as indicated by the hollandite structure-type. It is tempting, therefore, to speculate that when the todorokite structure is eventually solved towards the 21st century, this Mn^{IV} oxide may have one of the futuristic structures illustrated in figure 7, such as that of the $Na_xFe_xTi_{2-x}O_4$ phase, which has cell parameters analogous to those of todorokite.

Crystal chemistry of manganese nodules

A large number of elements are enriched in manganese nodules relative to their abundances in seawater or 'average' crust. They include the transitions metals Mn, Fe, Co, Ni, and Cu, as well as Zn, Mo, Ba, and Pb. Many of these metals are also enriched in terrestrial manganese oxide minerals or, along with Na, K, and Ca, form discrete phases with manganese (table 1). In order to understand the relative enrichment of these elements in hydrated manganese oxide or iron oxyhydroxide phases, it is necessary first to establish the oxidation states of each element and stabilization energy of each cation. Crystal field stabilization energies and radius ratio criteria result in transition metal ions favouring octahedral sites in oxide structures (Burns 1970). The larger cations K^+, Ba^{2+}, Pb^{2+}, Ca^{2+}, and Na^+, on the other hand, predominate in sites with higher coordination numbers, such as the cavities found in the hollandite and psilomelane structures (figures 3, 4).

Since manganese nodules form in oxidizing environments, cations with higher valencies predominate over reduced oxidation states. Indeed, results of Mössbauer studies (Carpenter & Wakeham 1973) show that iron occurs principally as Fe^{3+} ions in manganese nodules, while e.s.r. and e.s.c.a. measurements indicate the presence of only small amounts of Mn^{2+} ions. Spectroscopic techniques have not been developed to the extent of being able to identify the oxidation states of Co, Ni, and Cu in the nodules. As a result, inter-element relationships derived from microprobe measurements have been used to deduce the valencies of these elements in manganese nodules. Most nodules show strong positive correlations between Mn, Ni, Cu, and Zn, suggesting that the divalent cations Ni^{2+}, Cu^{2+}, and Zn^{2+} substitute for Mn^{2+} in todorokite and birnessite host phases. Some nodules show a correlation between Mn and Co, suggesting the presence of Co^{2+} ions. Other nodules show a well-defined apparent Fe–Co correlation, which has been interpreted as Co^{3+} substituting for Fe^{3+} ions in the $FeOOH.xH_2O$ phase (Burns 1965). Thermodynamic arguments (Burns 1976) support the existence of Co^{III} in the marine environment. It is noteworthy that Co^{3+} ions have a low-spin configuration in oxide structures, and that the ionic radius of Co^{3+} (52.5 pm) is considerably smaller than Fe^{3+} (64.5 pm), so that cobalt may not be tolerated in the $FeOOH.xH_2O$ phase. In fact, the mineral heterogenite, CoOOH, is not isostructural with any of the FeOOH polymorphs. On the other hand, the radius of Co^{3+} is similar to that of Mn^{4+} (54 pm). Therefore, the strong fractionation of cobalt into synthetic, terrestrial, and marine manganese oxide phases may be the result of Co^{3+} substituting for Mn^{4+} ions in the $[MnO_6]$ octahedra, leading to a very high crystal field stabilization energy for cobalt (Burns 1976). Therefore, the most likely cations occurring in manganese nodules are Mn^{4+}, Fe^{3+}, Co^{3+}, Ni^{2+}, Cu^{2+}, and Zn^{2+}, with smaller proportions of Mn^{2+}, Mn^{3+}, and Co^{2+}, and negligible amounts of Fe^{2+}.

The uptake of cobalt, nickel, and copper into the host ferromanganese oxide phases of manganese nodules may be interpreted as follows. The birnessite phase accommodates Ca^{2+}, Mn^{2+}, and Na^+ ions between the sheets of $(H_2O + OH^-)$ groups and layers of edge-shared $[MnO_6]$ octahedra (compare the chalcophanite structure shown in figure 5*a*). The divalent transition metals contained in seamount manganese nodules are probably situated in these between-layer sites of birnessite. However, by analogy with chalcophanite which appears to accommodate some Mn^{2+} ions in the Mn^{4+} sites, a portion of the Ni^{2+} and Cu^{2+} cations in birnessite may also be present in the layers of edge-shared $[MnO_6]$ octahedra. The smaller Co^{3+} ions, on the other hand, are much more readily accommodated in the octahedral Mn^{4+}

PHILOSOPHICAL TRANSACTIONS OF THE ROYAL SOCIETY A MATHEMATICAL, PHYSICAL & ENGINEERING SCIENCES

sites or in vacancies in the [MnO_6] layers of birnessite *and* the disordered δ-MnO_2 phase, thus accounting for the uptake, fixation, and enrichment of cobalt in soils and in manganese nodules from seamounts (Burns 1976). Some of the Pb, as well as Ce and Mo found in nodules, may also occur as tetravalent cations substituting for Mn^{4+} in the linked [MnO_6] octahedra.

Although the todorokite structure is unknown, this mineral does appear to contain essential Mn^{2+} ions, and probably has some form of linkage with chains of edge-shared [MnO_6] octahedra, possibly resembling the framework structures of hollandite, psilomelane, and certain Ti^{IV} oxides. Therefore, divalent nickel, copper, and zinc probably replace the Mn^{2+} ions in sites which bear similarities to the M_2 octahedra of the psilomelane structure (figure 4). Small amounts of Co^{3+} may also replace Mn^{4+} ions in the [$Mn^{IV}O_6$] octahedra resembling the psilomelane M_1 and M_3 sites. The uptake of large cations such as Ba^{2+}, K^+, and perhaps Pb^{2+}, into manganese nodules, as well as substantial amounts of water, suggests the presence of a phase similar to hollandite and psilomelane having large cavities in the framework of edge-shared [MnO_6] octahedra.

Nucleation and authigenesis of manganese nodules

There is abundant evidence summarized in the previous section that crystal structure is a major factor in controlling the uptake of metals into manganese nodules. The crystalline ferromanganese oxide phases contain sufficient coordination sites to accommodate favourably and stabilize the transition metal ions Mn^{4+}, Mn^{3+}, Fe^{3+}, Co^{3+}, Co^{2+}, Ni^{2+}, and Cu^{2+}. The question arises whether structural factors control the growth of the host phases. Recently, hypotheses on the mechanism of nucleation and authigenesis of many nodules (Burns & Brown 1972; Burns & Burns 1975; Burns *et al.* 1974) have been proposed and are summarized as follows.

Orange-brown coatings of iron oxyhydroxide phases are frequently observed on substrates such as foraminifera tests, coral, sharks' teeth, palagonite, phillipsite, and other secondary phases associated with altered volcanic rocks. The chemical constituents of these substrates contain anion radicals derived from weak acids (e.g. carbonates, phosphates, silicates), suggesting that $FeOOH.xH_2O$ was precipitated when locally high pH's were produced in seawater trapped in cavities during solution and hydrolysis of the substrate. After the precipitation of $FeOOH.xH_2O$ reaches an advanced stage of deposition, incipient brown-black coatings of manganese(IV) oxide become visible. Electron microprobe traverses across the boundary between the manganese oxide growth and the nucleus frequently show coronae of iron preceding the manganese deposit (Burns & Brown 1972). Such evidence for the growth of manganese(IV) oxide on the $FeOOH.xH_2O$ layer, together with the fact that manganese nodules always contain major proportions of manganese and iron, suggests that there are crystallographic relationships between the Mn and Fe phases which allow contemporaneous or cyclic structural intergrowths.

The tabulations of oxide minerals of manganese and iron in tables 1 and 2 show the existence of isostructural minerals of Mn and Fe, notably ramsdellite and goethite, hollandite group and akaganéite, and probably δ-MnO_2 and $FeOOH.xH_2O$. In such pairs of minerals having identical crystal structures, or layers of atoms in common in a specific crystallographic plane, the possibility exists for orientated intergrowths of one crystalline phase with the other, provided there is a similarity of lattice parameters or interplanar spacings. An excellent example of

PHILOSOPHICAL TRANSACTIONS OF THE ROYAL SOCIETY A MATHEMATICAL, PHYSICAL & ENGINEERING SCIENCES

such epitaxial growth is ramsdellite (MnO_2) crystallites which can be seen by s.e.m. to grow in crystallographic continuity with goethite (α-FeOOH) (Finkelmann *et al.* 1972, 1974). There is less than 10 % mismatch of cell parameters between the smaller ramsdellite unit cell and the goethite structure (tables 1 and 2). This mismatch is sufficiently small to permit epitaxial intergrowth of the two phases perpendicular to the layers of hexagonally close-packed oxygen atoms.

Although δ-MnO_2 and $FeOOH.xH_2O$ consist of very small, disordered crystallites, both phases contain cations in octahedral sites of hexagonally close-packed oxygen layers. Therefore, these two phases in manganese nodules are highly susceptible to epitaxial intergrowths, which probably initiates nucleation and leads to the intimate association of Mn and Fe oxide phases. This intergrowth of δ-MnO_2 and $FeOOH.xH_2O$ inhibits the formation of the ordered layer structure of birnessite. However, local enrichments of divalent cations (Ca^{2+}, Ni^{2+}, Cu^{2+}, Mn^{2+}) breaks the sequence of oscillatory intergrowths of δ-MnO_2 and $FeOOH.xH_2O$ and leads to the development of birnessite or todorokite crystallites.

Towards the 21st century

Progress in manganese nodule mineralogy has paralleled developments in solid-state chemistry and physics. As high resolution techniques have evolved during the 20th century, so too has the characterization of the manganese oxide phases. We have come a long way in the past 100 years from simply classifying the nodules as manganiferous wads and regarding them as museum curiosities. Sophisticated electronics equipment, such as electron microprobes and scanning electron microscopes equipped with X-ray energy dispersive analytical accessories, now permit more detailed microchemical and morphological characterization of the submicroscopic minerals hosting the strategic metals Co, Ni, and Cu in the manganese nodules.

As electron microscopy and higher resolution techniques are developed during the next 100 years, the likelihood exists that cryptocrystalline fragments associated with the complex, fragile structures of several manganese(IV) oxides may be recognized in manganese nodules. Such discoveries will permit more rigorous interpretations of the crystal chemistry and bonding of transition metals in marine manganese nodules.

Research on the crystal chemistry and mineralogy of manganese nodules is supported by a grant from the NSF–IDOE Seabed Assessment Program, Manganese Nodule Project (Grant No. IDO75-12957). We thank Ms Roxanne Regan for the preparation of the manuscript.

References (Burns & Burns)

Brown, F. H., Pabst, A. & Sawyer, D. L. 1971 Birnessite on colemanite at Boron, California. *Am. Miner.* **56**, 1057–1064.

Burns, R. G. 1965 Formation of cobalt(III) in the amorphous $FeOOH.nH_2O$ phase of manganese nodules. *Nature, Lond.* **205**, 999.

Burns, R. G. 1970 *Mineralogical applications of crystal field theory*. Cambridge University Press.

Burns, R. G. (ed.) 1975 Symposium on manganese in the sea and the Manganese Nodule Project. *EOS* (*Trans. Am. Geophys. Un.*) **56**, 998–1000.

Burns, R. G. 1976 The uptake of cobalt into ferromanganese nodules, soils, and synthetic manganese(IV) oxides. *Geochim. cosmochim. Acta* **40**, 95–102.

PHILOSOPHICAL TRANSACTIONS OF THE ROYAL SOCIETY A MATHEMATICAL, PHYSICAL & ENGINEERING SCIENCES

Burns, R. G. & Brown, B. A. 1972 Nucleation and mineralogical controls on the composition of manganese nodules. In D. R. Horn (editor), *Ferromanganese deposits on the ocean floor* (ed. D. R. Horn), pp. 51–61. Washington, D.C.: NSF–IDOE Publ.

Burns, R. G. & Burns, V. M. 1975 Mechanism for nucleation and growth of manganese nodules. *Nature, Lond.* **255**, 130–131.

Burns, R. G. & Burns, V. M. 1977*a* Mineralogy of ferromanganese nodules. In *Marine manganese deposits* (ed. G. P. Glasby), chapter 7. (In the press.)

Burns, R. G., Burns, V. M., Sung, W. & Brown, B. A. 1974 Ferromanganese nodule mineralogy: suggested terminology of the principal manganese oxide phases. *Geol. Soc. Am., Ann. Meet., Miami, Abstr.* **6**, 1029–1031.

Burns, R. G. & Fuerstenau, D. W. 1966 Electron-probe determination of inter-element relationships in manganese nodules. *Am. Miner.* **51**, 895–902.

Burns, V. M. & Burns, R. G. 1977*b* Post-depositional metal enrichment processes inside manganese nodules from the north equatorial Pacific. *Nature, Lond.* (In the press.)

Buser, W. 1959 The nature of the iron and manganese compounds in manganese nodules. *Int. Oceanogr. Congr., AAAS*, pp. 962–963.

Buser, W. & Grütter, A. 1956 Über die Natur der Manganknollen. *Schweiz. Mineral. Petrogr. Mitt.* **36**, 49–62.

Byström, A. M. 1949 The crystal structure of ramsdellite, an orthorhombic modification of MnO_2. *Acta Chem. Scand.* **3**, 163–173.

Byström, A. & Byström, A. M. 1950 The crystal structure of hollandite, the related manganese oxide minerals, and α-MnO_2. *Acta Cryst.* **3**, 146–154.

Carpenter, R. & Wakeham, S. 1973 Mössbauer studies of marine and fresh water manganese nodules. *Chem. Geol.* **11**, 109–116.

Chukhrov, F. V., Zvyagin, B. B., Gorshkov, A. I., Yermilova, L. P. & Balashova, V. V. 1973 On ferrihydrite (hydrous ferric oxide). *Akad. Nauk. SSSR, Ser. Geol.* **4**, 23–33.

Clark, G. M. 1972 *The structures of non-molecular solids.* London: Applied Science Publ.

Cronan, D. S. & Tooms, J. S. 1968 A microscopic and electron probe investigation of manganese nodules from the northwest Indian Ocean. *Deep-Sea Res.* **15**, 215–223.

Dugolinsky, B. K. & Margolis, S. V. 1976 Encrusting protozoans contribute to growth of manganese nodules. *Science, N.Y.* (In the press.)

Ehrlich, H. L. 1963 Bacteriology of manganese nodules. *Appl. Microbiol.* **11**, 306–310.

Finkelman, R. B., Matzko, J. J., Woo, C. C., White, Jr, J. S. & Brown, W. R. 1972 A scanning electron microscopy study of minerals in geodes from Chihuahua, Mexico. *Miner. Rec.* **3**, 205–212.

Finkelman, R. B., Evans, Jr., H. T. & Matzko, J. J. 1974 Manganese minerals in geodes from Chihuahua, Mexico. *Miner. Mag.* **39**, 549–558.

Gallagher, K. J. 1970 The atomic structure of tubular subcrystals of β-iron(III) oxide hydroxide. *Nature, Lond.* **226**, 1225–1228.

Giovanoli, R. & Burki, P. 1975 Composition of X-ray evidence of marine manganese nodules and non-marine manganese ore deposits. *Chimia* **29**, 266–269.

Giovanoli, R., Bühler, H. & Sokolowska, K. 1973 Synthetic lithiophorite: electron microscopy and X-ray diffraction. *J. Microsc.* **18**, 271–284.

Giovanoli, R., Feitknecht, W. & Fischer, F. 1971 Über Oxidhydroxide des vierwertigen Mangans mit Schichtengitter. 3. Reduction von Mangan(III)–Manganat(IV) mit Zimtalkohol. *Helv. chim. Acta* **54**, 1112–1124.

Giovanoli, R., Stahli, E. & Feitknecht, W. 1970*a* Über Oxidhydroxide des vierwertigen Mangans mit Schichtengitter. 1. Natrium-mangan(II, III) Manganat(IV). *Helv. chim. Acta* **53**, 209–220.

Giovanoli, R., Stahli, E. & Feitknecht, W. 1970*b* Über Oxidhydroxide des vierwertigen Mangans mit Schichtengitter. 2. Mangan(II)–Manganat(IV). *Helv. chim. Acta* **53**, 453–464.

Glasby, G. P. (ed.) 1977 *Marine manganese deposits.* Amsterdam: Elsevier Publ. Co. (In the press.)

Graham, J. W. & Cooper, S. C. 1959 Biological origin of manganese-rich deposits on the sea floor. *Nature, Lond.* **183**, 1050–1051.

Greenslate, J. 1974*a* Microorganisms participate in the construction of manganese nodules. *Nature, Lond.* **249**, 181–183.

Greenslate, J. 1974*b* Manganese and biotic debris associations in some deep-sea sediments. *Science, N.Y.* **186**, 529–531.

Hey, M. H. & Embrey, P. G. 1974 Twenty-eighth list of new mineral names. *Miner. Mag.* **39**, 903–932.

Horn, D. R. (ed.) 1972 Ferromanganese deposits on the ocean floor. Office for the International Decade of Ocean Exploration, NSF, Washington, D.C.

Horn, D. R., Horn, B. M. & Delach, M. N. 1973 Ocean manganese nodules metal values and mining sites. *Tech. Rep.* no. 4, NSF GX-33616, Washington, D.C.

Hubred, G. 1975 Deep-sea manganese nodules: a review of the literature. *Minerals. Sci. Engng* **7**, 71–85.

Manheim, F. T. 1965 Manganese-iron accumulations in the shallow marine environment. In *Symposium on marine chemistry* (eds D. R. Schink & J. T. Corliss), vol. 3, pp. 217–276. Occas. Publ., Univ. Rhode Island.

Margolis, S. V. & Burns, R. G. 1976 Pacific deep-sea manganese nodules: their distribution, composition, and origin. *A. Rev. Earth Planet. Sci.* **4**, 229–263.

PHILOSOPHICAL TRANSACTIONS OF THE ROYAL SOCIETY A MATHEMATICAL, PHYSICAL & ENGINEERING SCIENCES

Mero, J. L. 1965 *The mineral resources of the seas*. Amsterdam: Elsevier.
Morganstein, M. (ed.) 1973) *The origin and distribution of manganese nodules in the Pacific and prospects for exploration*. Publ. by Hawaii Inst. Geophys. and NSF–IDOE.
Mumme, W. G. 1968 The structure of $Na_4Mn_4Ti_5O_{18}$. *Acta Cryst.* **B24**, 1114–1120.
Mumme, W. G. & Reid, A. F. 1968 Non-stoichiometric sodium iron titanate, $Na_xFe_xTi_{2-x}O_4$, $0.90 > x > 0.75$. *Acta Cryst.* **B24**, 625–631.
Mumme, W. G. & Wadsley, A. D. 1967 The crystal structure of $NaTi_2Al_5O_{12}$. *Acta Cryst.* **23**, 754–758.
Murray, J. & Irvine, R. 1894 On the manganese oxides and manganese nodules in marine deposits. *Trans. R. Soc., Edin.* **37**, 712–742.
Murray, J. & Renard, A. 1891 Report on deep-sea deposits. In *Report on the scientific results of the voyage of H.M.S. 'Challenger'* (ed. C. Wyville Thomson), vol. 5. London: Eyre & Spottiswoode.
Ostwald, J. & Frazer, F. W. 1973 Chemical and mineralogical investigations on deep-sea manganese nodules from the Southern Ocean. *Miner. Deposita* **8**, 303–311.
Oswald, H. R. & Wampetich, M. J. 1967 Die Kristallstrukturen von Mn_5O_8 und $Cd_2Mn_3O_8$. *Helv. chim. Acta* **50**, 2023–2034.
Sisselman, R. 1975 Ocean miners take soundings on legal problems, development alternatives. *Eng. Mining J.* April, 75–86.
Sorem, R. K. & Foster, A. R. 1972 Marine manganese nodules: importance of structural analysis. *Proc. 24th Int. Geol. Congr.*, Sect. 8, 192–200.
Sorokin, Y. I. 1972 Role of biological factors in the sedimentation of iron, manganese, and cobalt and the formation of nodules. *Oceanology* **12**, 1–11.
Straczek, J. A., Horen, A., Ross, M. & Warshaw, C. M. 1960 Studies of the manganese oxides. IV. Todorokite. *Am. Miner.* **45**, 1174–1184.
Wadsley, A. D. 1952 The structure of lithiophorite (Al, Li)$MnO_2(OH_2)$. *Acta Cryst.* **5**, 676–680.
Wadsley, A. D. 1953 The crystal structure of psilomelane, $(Ba, H_2O)_2Mn_5O_{10}$. *Acta Cryst.* **6**, 433–438.
Wadsley, A. D. 1955 The crystal structure of chalcophanite, $ZnMn_3O_7.3H_2O$. *Acta Cryst.* **8**, 165–172.
Woo, C. C. 1973 Scanning electron micrographs of marine manganese micronodules, marine pebble-sized nodules, and fresh water manganese nodules. In *The origin and distribution of manganese nodules in the Pacific and prospects for exploration* (ed. M. Morganstein). Publ. Hawaii Inst. Geophys. and NSF–IDOE.

Discussion

A. J. Easton (*British Museum (Natural History), Cromwell Road, London SW7 5BD*). Have adjacent nodules been examined, and if so do you obtain similar spectra for trace elements?

R. G. Burns. We have examined about 20 manganese nodules from the north equatorial Pacific using electron microprobe and scanning electron microscope techniques (Burns 1975 and *Geol. Soc. Am., Ann. Meet. Abstr.* 1975 **7**, 1014). The microprobe analyses show that the metal concentrations fluctuate widely across sectioned nodules, but conform with the well-known positive Mn–Ni–Cu and negative Mn–Fe interelement correlations. Individual growth bands 1–10 μm in diameter may contain as much as 30–40 % Mn (by mass) plus 4–5 % Ni and 3–4 % Cu. We have discovered that the positions of certain bands richest in (Ni + Cu) appear to be displaced towards the nodule exterior the further westward along the north equatorial Pacific belt from which the nodule was collected. At one station (11° N, 140° W), chemical stratigraphic correlations appear to exist between different manganese nodules. Observations by scanning electron microscopy indicate that metal-rich areas in interiors of manganese nodules may be correlated with post-depositional recrystallization textures.

PHILOSOPHICAL TRANSACTIONS OF THE ROYAL SOCIETY A MATHEMATICAL, PHYSICAL & ENGINEERING SCIENCES